

Simulation study on automotive EMB system based on self-tuning fuzzy PID control

LIJUN XIE¹, WENHUI YANG^{1,2}

Abstract. To enhance stability of automobile brake, and shorten brake distance, study is made on anti-lock control and its control theory based on electronic mechanical brake system (EMB system). Models related to EMB system was built according to dynamics analysis for automobile braking system, and simulation was made to those models under Anti-Lock Braking System (ABS System). Then, self-tuning fuzzy PID controller was put forward to improve fuzzy control and PID control. Comparison was made between braking mode that without ABS control and self-tuning fuzzy PID. Finally, pavement simulation was made in order to verify the adaptiveness of self-tuning fuzzy PID controller. The results showed that models related to EMB system are effective and have met the national standard and code for braking system. Automobile braking performance was improved because fuzzy control and PID control was improved by self-tuning fuzzy PID control. And it is concluded that self-tuning fuzzy PID controller is good at identify pavement types which meets the control requirement and expectations.

Key words. Self-tuning fuzzy PID control, EMB, ABS, slip rate.

1. Introduction

The braking system is one of the most important parts of an automobile. Its main function is: first of all, to ensure stable parking at high speed, and when accidents occur, it is very important to its performance requirements. Secondly, its function is to ensure that the vehicles, in the event of poor road conditions and when necessary to reduce the speed, can slow down the parking; or in downhill road, when necessary to travel at a constant speed, to ensure that the brake has high reliability and does not fail due to friction sheet overheating [1–3]. The last one is the parking function. Parking is, with a constant braking force, to ensure that the vehicles stay in place after the end of driving, and do not move because of terrain and other reasons. These are the functions that the braking system should have.

¹Changsha Vocational & Technical College, 410217, China

²Corresponding author

The braking system is mainly composed of a drive mechanism and a brake actuating mechanism. The braking transmission mechanism can be divided into mechanical transmission and hydraulic transmission in accordance with the transmission mode. The simple mechanical drive is seldom used at present, and hydraulic transmission is the most widely used transmission method [4–6]. However, with the development of intelligent systems, the number of electronic control systems is gradually increasing, which makes the hydraulic system with pipeline transmission become more complex and difficult to maintain. Therefore, it has become an important problem for people to study a kind of system with simple structure and reliable function.

As one of the most important performances for automobile, automobile braking performance, such as braking distant, side slipping and braking direction, is responsible for traffic accident. Under certain braking initial speed, braking distant is related to two factors, brake response time and wheels' utilization rate of pavement deceleration. Overall circuit transfer was used by EMB, thus response time for braking controller braking distant is shortened [7]. Braking distant is further shortened by adopting effective ABS control because pavement adhesion is used to the highest degree [8]. In terms of intelligence and safety, system structure is simplified by adopting CAN and EMB, because of which fault detection and maintenance is more convenient. Thus, fault detection and maintenance for braking system is improved [9]. In conclusion, security of automobile control can be ensured by adopting improved EMB system.

2. State of the art

Originally, EMB system is used for plane [10], and this system is in the improvement stage for automobile field. Significant achievements for study and application of fuzzy theory are mainly made in America or countries and regions in European. For research results on fuzzy ABS, slip rate predictor is introduced by Georg E. Mauer [11] and his partners based on ABS controller. Using this slip rate predictor, good control is achieved in simulation for single wheel model, and robustness is improved. Model-based control methods such as PID controller and fuzzy controller, was combined by R. Sun [12] and this controller combination verified that adaptability to different pavement is improved comparing with PID controller. Robust controller is built by Chin-Min Lin and his partners based on fuzzy controller. Certain control effects are made when fuzzy controller is adopted for braking control and robust controller is adopted for adjusting control errors of fuzzy control [13]. Regarding research status at home and abroad, there are disadvantages in fuzzy control though great progresses are achieved. Thus, further study and discussion is needed theoretically and pragmatically.

Compared with foreign countries, the application of fuzzy theory in our country started relatively late, but it has developed rapidly. In recent years, many universities and automobile research institutions in China have done a great deal of theoretical and experimental researches on ABS fuzzy control technology, which laid the foundation for the development of ABS fuzzy control in our country. The famous scholar Guo Konghui, based on the simplified model, designed the fuzzy controller

and the adaptive fuzzy controller. As a result, the vehicle can achieve better control in variable conditions, which overcomes the shortcomings of single control and so on. Li Jun, Yu Fan, Zhang Jianwu and other scholars proposed control strategy of road recognition in the process of steering braking. The strategy, according to the road adhesion conditions and the motion state, the vehicle pavement condition was estimated, wheel optimal slip ratio was real-time calculated, and the corresponding control strategies were made, so the braking and vehicle lateral stability was greatly improved. Mo Yousheng, Zhu Rong and Li Sien put forward adaptive fuzzy neural network control system with combination of fuzzy control and neural network control. In addition, it was compared with the fuzzy control, and the simulation was made to verify the validity of the control. Chen Jiong, Wang Huiyi and Song Jian designed a fuzzy controller based on slip ratio and speed reduction. The simulation was carried out on a vehicle model of freedom, and it was proved that the controller is more adaptive than the logic threshold method.

From the present research situation at home and abroad, although fuzzy control has been greatly developed, there is still a lack of fuzzy control. For instance, the creation and analysis methods of fuzzy control system were still in the primary stage, and the stability theory was not mature. In addition, the modeling of fuzzy systems, establishment of fuzzy rules and fuzzy inference methods were also not well resolved. As a result, both theory and application need to be further studied and discussed.

3. Methodology

3.1. Dynamics modeling for EMB

Automobile EMB system is mainly made up of electronic pedal, electronic control unit (ECU), wheel braking system, and power [14, 15]. A set of braking system and wheel speed sensor (WSP) is installed on each wheel of the automobile. Each braking system contains a control unit (CU) to control performance of electric machine and the needed control signals is provided by ECU [16, 17]. For general structure, see Fig. 1.

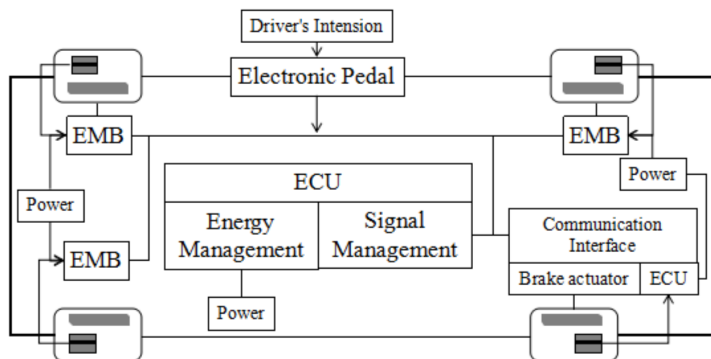


Fig. 1. General structure of EMB system

External force is needed to decelerate or stop automobile in a short time [18]. Among external forces, braking force is one of the most important one to decelerate automobile. Thus, braking performance is studied and this study is mainly focused on effectiveness of braking force to automobile movement.

When wheel braking on hard pavement, rolling friction couple, inertia force and inertia couple occurred during deceleration were ignored. Figure 2 shows stress state of wheel.

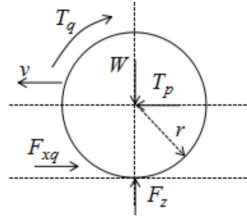


Fig. 2. Stress state of wheel during braking

In the above figure, T_q denotes braking torque (N·m) of brake, T_p denotes thrust of driving direction of wheel, F_q denotes braking force, F_{xq} denotes braking force of the pavement, W denotes loads of wheel F_z denotes normal reaction of pavement to wheel, r denotes action radius of wheel. Thus, the below equation is obtained.

$$F_{xq} = F_q = \frac{T_q}{r}. \quad (1)$$

During automobile braking, friction plate gradually touches brake disc with increasing braking force. At this state, T_q is not big enough to lock wheel. This is called state of friction and rolling. Under this state, pavement brake torque equals to T_q , and pavement brake torque is in direct proportion to T_q . When T_q keeps increasing, there is only friction state for wheel. At this state, pavement brake force is no longer in direct proportion to T_q , and its limit value is the adhesive force F_ϕ , see the below equality

$$F_{xq} \leq F_\phi = F_{z\phi}. \quad (2)$$

During braking, state of wheel is changed from rolling to lock and slipping. In this state, wheel is rolling and slipping, and slipping is decided by slip rate. The below expression

$$S = \frac{v - v_r}{v} \times 100\% = \frac{v - r\omega}{v} \times 100\% \quad (3)$$

shows slip rate.

In the above expression, v denotes the automobile speed, v_r denotes the wheel speed and ω denotes the angular speed of wheel. In the rolling state, $v = v_r$, thus $S = 0$. In state of rolling and slipping, $0 < S < 100\%$. In locked friction state, $v_r = 0$ and $S = 100\%$. Steering capability of automobile is lost, which is very dangerous working state.

Modeling on automobile brake system based on above dynamics analysis. Mathematical model about automobile brake system is mainly made up of vehicle dynamics

model, tire model, and brake system model.

3.1.1. Dynamics model of single wheel vehicle. In order to verify controller performance and highlight its control law, a single wheel automobile is studied. Vehicle dynamic functions of two-degree-of-freedom is built based on wheel driving direction and direction of rotating around principle axis.

Vehicle movement function is

$$M\dot{v} = -F_{xq}. \quad (4)$$

Wheel movement function is

$$I\dot{\omega} = rF_{xq} - T_q \quad (5)$$

and the longitudinal friction of wheel is

$$F_{xq} = \phi F_z. \quad (6)$$

In the above expressions, M denotes 1/4 of the vehicle weight, F_{xq} denotes the cohesion force of tire to pavement and I denotes the rotational inertia of the wheel. Finally F_z denotes the normal reaction of pavement to wheel.

3.1.2. Tire model. Tire is the only part of vehicle that contact with pavement, and its cohesion to pavement, and its driving force, braking force, and trafficability to vehicle is of significant influence. Tire model can be used to approximate rapid analyze vehicle controllability and stability theoretically. Tire model reflects function relationships between pavement cohesion and other parameters. The below bilinear model is used to study tire model.

The bilinear model is a simplified tire model. Relationship of slip rate and adhesion coefficient is nonlinear. For the convenient of function solving, bilinear model is piecewise linearized, see Fig. 3. The function for bilinear tire model is deduced according to Fig. 3. **Figure 3 is missing.**

$$\begin{cases} \varphi = \frac{\varphi_p}{S_o} S & , S < S_o \\ \varphi = \frac{\varphi_p - \varphi_s}{1 - S_o} S - \frac{\varphi_p - \varphi_s}{1 - S_o} S & , S > S_o \end{cases} \quad (7)$$

In the above function, S denotes the wheel slip rate, S_o denotes the optimal slip rate, φ_p denotes the maximum adhesion coefficient; φ_s denotes slip adhesion coefficient.

The simplified bilinear tire model is adopted, and Table 1 shows the parameters of experimental made on typical pavement.

3.1.3. Model for EMB braking system. A brushless direct current motor is adopted as motive power of EMB system. Mainly, electronic machine in locked-rotor state is studied, which is focused on wheel braking state. The below function shows relationship between locked-rotor current and control signal of electronic machine

Table 1. Parameters of experiments on typical pavement

Types of pavement	S_o	ϕ_p	ϕ_s	Bilinear model
Concrete pavement	0.2	0.89	0.76	$\begin{cases} \phi = 4.5S & , S < 0.2 \\ \phi = 0.92 - 0.19S & , S > 0.2 \end{cases}$
Dry bitumen pavement	0.16	0.82	0.76	$\begin{cases} \phi = 4.7S & , S < 0.16 \\ \phi = 0.82 - 0.29S & , S > 0.16 \end{cases}$
Wet bitumen pavement	0.13	0.78	0.52	$\begin{cases} \phi = 6S & , S < 0.13 \\ \phi = 0.83 - 0.32S & , S > 0.13 \end{cases}$
Pavement covered by snow	0.06	0.22	0.15	$\begin{cases} \phi = 3.3S & , S < 0.06 \\ \phi = 0.23 - 0.06S & , S > 0.06 \end{cases}$

$$I_c = k_c \cdot \alpha, \quad (8)$$

where I_c denotes locked-rotor current, k_c denotes conversion relations between control signals and locked-rotor current, α denotes inputted control signal. Below function shows relations between I_c and output torque of electronic machine.

$$T_m = 9.55k_G \cdot I_c, \quad k_G = \frac{E}{n_o}, \quad E = U_o - I_o r_o. \quad (9)$$

For the above function, T_m denotes the output torque of electronic machine, I_o denotes the non-load current, I_c denotes the current of locked-rotor, U_o denotes the non-load voltage of power, E denotes the counter electromotive force of the armature winding, r_o denotes the average resistance of armature winding, k_G denotes counter electromotive force coefficient, and n_o denotes the idle speed of electronic machine.

Planetary reducer is adopted by reducing mechanism model which is made up of sun wheel and planet carrier. T_m denotes input moment of sun wheel, and torque T_x denotes output planetary reducer. Below function shows the relations.

$$T_x = T_m \cdot i \cdot \eta_x, \quad (10)$$

where, i denotes transmission ratio of speed reducer, η_x and denotes transmission efficiency of planetary mechanism. Motion transfer device is made up of ball screw-nut pair. Finally, T_x denotes the input and P denotes outputted thrust of ball screw.

$$P = T_x \cdot \eta_g \cdot \frac{2\pi}{L_h}. \quad (11)$$

In the above formulas, L_h denotes lead of screw thread and η_g denotes transmission efficiency of ball screw. Ball screw and brake caliper were connected to each other and lining pad of brake caliper and brake disc are connected to each other through thrust P . Braking torque is produced due to friction of lining pad and brake disc. Below function shows relations between brake pressure and brake

moment when friction surface of lining pad and brake disc connects well.

$$T_q = 2P \cdot k_p \cdot R. \quad (12)$$

In above expression, k_p denotes brake friction coefficient, R denotes action radius, and P denotes the lead screw thrust. Table 2 shows the parameters of the used electric machine, and Table 3 shows the parameters of EMB brake actuator.

Table 2. Parameters of electric machine of permanent magnet DC motor

Parameter names	Non-load voltage (V)	Non-load current (A)	Armature resistance (Ω)	Non-load speed (r/min)	Locked-rotor current (A)	Maximum locked-rotor current (A)
Symbols	U_o	I_o	r_o	n_o	I_c	$I_{c \max}$
Values	27	0.30	3.68	491	2.2	7

Table 3. Parameter of EMB brake actuator

Symbols of parameters	i	η_x	L_h	η_g	k_p	R
Values	20	0.95	0.016	0.95	2	0.2

3.2. Modeling on brake system of electric mechanical machine

Matlab/Simulink is used to model and simulate subsystems. Without control of ABS, effectiveness of the EMB brake system is tested.

3.2.1. *Subsystem of single wheeled vehicle.* After solving functions (4), (5) and (6), below expressions for v , v_r and s can be obtained:

$$v = - \int \frac{F_{xq}}{M} dt, \quad v_r = \frac{r}{l} \int (rF_{xq} - T_q) dt, \quad s = - \int \left(\int \frac{F_{xq}}{M} dt \right) dt. \quad (13)$$

Simulation model of a single wheel can be built based on (13). With the input of T_q and F_{xq} , the curve of v and v_r changing with time can be obtained.

3.2.2. *Subsystem of slip rate.* Based on (3), subsystem of slip rate can be built. For this function, inputting v , v_r and adopting F_{cn} function, the slip rate of vehicle is output.

3.2.3. *Subsystem of tire model.* Simulation model is built based on bilinear calculation function (7), which inputs slip rate and outputs longitudinal adhesion coefficient.

3.2.4. *Subsystem of brake model.* Brake actuator is made up of brake transmission mechanism and brake, whose simulation module is built based on relations

(8–12), inputting control signal v , and outputting braking torque T_q .

3.3. Design of self-tuning fuzzy PID controller

Self-tuning fuzzy PID controller is the combination of fuzzy control and traditional PID control, which tunes PID control parameters online using fuzzy theory related knowledge. Intelligence of fuzzy control and sensitivity of PID control is integrated by this tuning. Figure 3 shows the system structure.

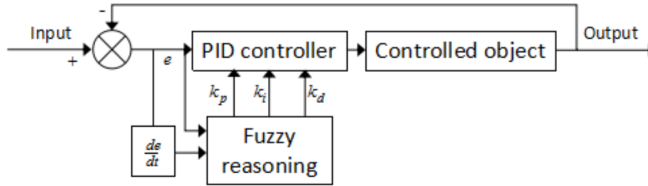


Fig. 3. Structure of self-tuning fuzzy system for automobile ABS

Self-tuning fuzzy PID controller is adjusting values of k_p , k_i , k_d in real time according to fuzzy control theory, thus objects is controlled. This controller inputs error e and its variation Δe , which is transmitted to E and ΔE after a fuzzy process. Symbols k_p^* , k_i^* , k_d^* are fuzzy set of output quantities k_p , k_i , k_d . For input quantities e and Δe , the universe of fuzzy set is $\{-3 - 2 - 1, 0, 1, 2, 3\}$, whose fuzzy language variables are $\{NB, NM, NS, ZO, PS, PM, PB\}$. For output quantities k_p^* , k_i^* , k_d^* , the universe of fuzzy set is $\{-3 - 2 - 1, 0, 1, 2, 3\}$, whose fuzzy language variables are $\{NB, NM, NS, ZO, PS, PM, PB\}$, which represent big negative, medium negative, small negative, zero, small positive, medium positive, and big positive, respectively.

The fuzzy control Table 4 is built based on characteristics without PID control and different e and Δe input by the system.

4. Results analysis and discussion

5. Test on effectiveness of system model of electronic mechanical brake system

Concrete pavement with relatively high adhesive force is used to test brake performance of EMB. Relatively strong brake force can be produced on concrete pavement. Table 5 shows the vehicle parameters.

It can be seen from Fig.4 that in the initial braking phase, pavement braking torque is in direct proportion to T_q while pavement braking torque is in inverse proportion to T_q after reaching its value. Without ABS control, adhesive coefficient is decreasing with the rapid increasing slip rate of wheel, thus ground adhering moment is decreased. When T_q keeps increasing, ground adhering brake moment will remain the same torque value with that of in slipping state.

Table 4. Rule list of fuzzy control for k_p^* , k_i^* and k_d^*

k_p^*							
	NB	NM	NS	ZO	PS	PM	PB
NB	PB	PB	PM	PM	PS	ZO	ZO
NM	PB	PB	PM	PS	PS	ZO	NS
NS	PM	PM	PM	PS	ZO	NS	NS
ZO	PM	PM	PS	ZO	NS	NM	NM
PM	NS	ZO	NS	NM	NM	NM	NB
PB	PB	ZO	NM	NM	NM	NM	NB
k_i^*							
	NB	NM	NS	ZO	PS	PM	PB
NB	NB	NB	NM	NM	NS	ZO	ZO
NM	NB	NB	NM	NS	NS	ZO	ZO
NS	NB	NM	NS	NS	ZO	PS	PS
ZO	NM	NM	NS	ZO	PS	PM	PM
PS	NM	NS	ZO	PS	PS	PM	PB
PM	ZO	ZO	PS	PS	PM	PB	PB
PB	ZO	ZO	PS	PM	PM	PB	PB
k_d^*							
	NB	NM	NS	ZO	PS	PM	PB
NB	PS	NS	NB	NB	NB	NM	PS
NM	PS	NS	NB	NM	NM	NS	ZO
NS	ZO	NS	NM	NM	NS	NS	ZO
ZO	ZO	NS	NS	NS	NS	NS	ZO
PS	ZO	ZO	ZO	ZO	ZO	ZO	ZO
PM	PB	NS	PS	PS	PS	PS	PB
PB	PB	PM	PM	PM	PS	PS	PB

Table 5. Parameters of single wheel vehicle

Name	1/4 Vehicle weight (kg)	Wheel radius (m)	Wheel rotary inertia (kg·m ²)	Gravitational acceleration (m/s ²)	Initial speed of braking (m/s)
Symbols	M	r	I	g	v
Values	1880	0.53	20	9.8	24

It is known from above simulation experiment that the wheel was locked in the 1.28 s after emergent brake under EMB brake system. Braking distance is 16.24 m, braking time is 2.34 s and the maximum vehicle deceleration is 8.85 m/s². Besides, the average deceleration is 7.16 m/s², and average braking coordination time is 0.14 s. This meets the national standard that requires coordination time should less than 0.35 s under such working state. Thus, EMB brake meets national requirement for braking performance well.

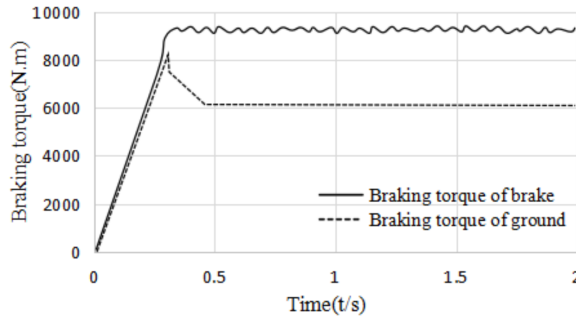


Fig. 4. Changes of braking torque of ground and brake without ABS control

5.1. Automobile ABS simulation based on self-tuning fuzzy PID control

Figure 5 shows automobile ABS simulation model built based on self-tuning fuzzy PID control.

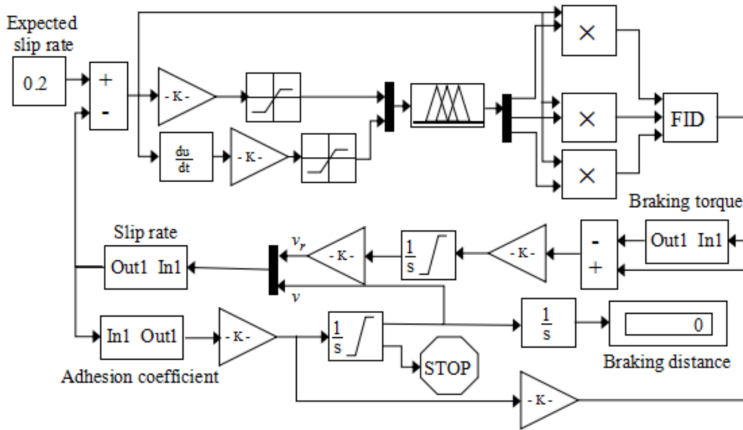


Fig. 5. Automobile ABS simulation model built based on self-tuning fuzzy PID control

In order to test the effectiveness of self-tuning fuzzy PID controller, comparison was made between braking systems with self-tuning fuzzy PID controller and system without ABS controller. Concrete pavement is chosen to be studied, with expected slip rate of 0.2, slip adhesion coefficient of 0.75, and initial braking speed of 24 m/s. Table 1 shows simulation parameters and Figs. 6 and 7 show the simulation results.

It can be seen from simulation results in Figs. 6 and 7 that the vehicle braking distance is 37.26 m and braking time is 3 s when the initial speed is 24 m/s. During braking, shown as Fig. 6, upper part, the slip rate remains the same as that of in 0.2 s and reaches its maximum in 0.3 s when without ABS control. It is shown on Fig. 6, bottom part, that without ABS control, vehicle speed is 23 m/s when wheel is locked. While under self-tuning fuzzy PID control, the wheel is locked when vehicle

speed is 0 m/s, which improves the braking stability. For Fig. 7, upper part, under ABS control, vehicle speed remains unchanged when it hits the highest deceleration 8.85 m/s^2 . Comparing vehicle speed without ABS control, this takes full advantages of ground adhesion. Besides, under fuzzy control, the braking distance is shortened by 7.41 m, and braking time is shortened by 0.62 s. In the whole braking process, it is shown in Fig. 7, bottom part, that the output is relatively stable. Thus, self-tuning fuzzy PID controller meets the ABS control goal and requirements of safety compared with the state without ABS control.

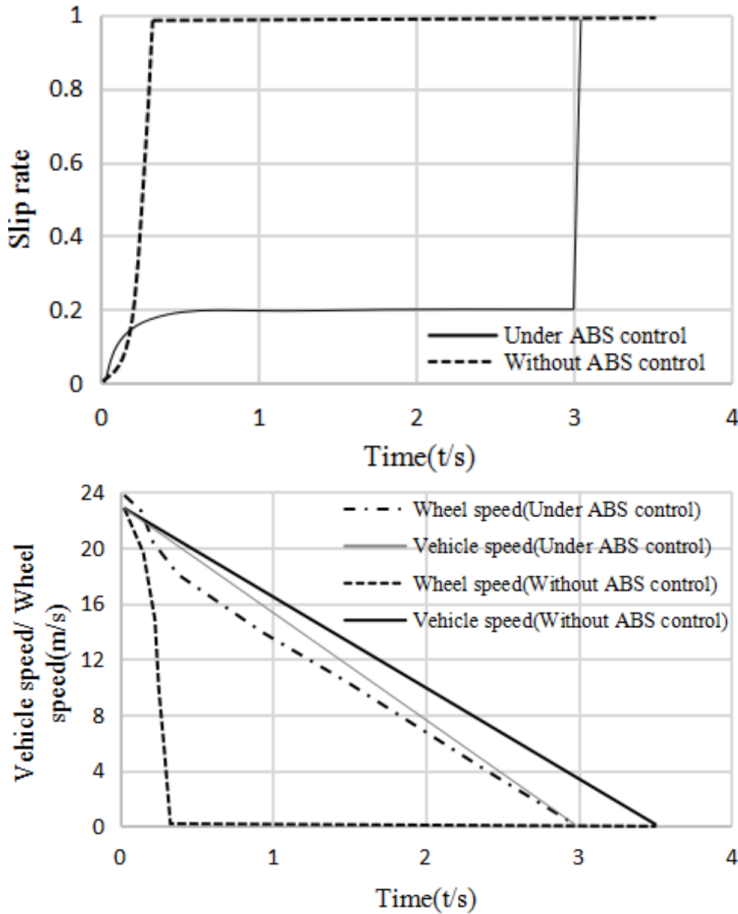


Fig. 6. Slip rate (up) and vehicle speed (bottom) for system with self-tuning fuzzy PID control and system without ABS control

The simulation and analysis was made based on bitumen pavement and pavement covered by snow. It is known that, in the 0.5 s, slip rate hits its optimal record of 0.06 and remains good stability when braking on the pavement covered by snow. In the 2 s after braking, when changing from pavement covered by snow to bitumen pavement, slip rate is unstable, which changed back to stable states 1 s later and

remains stable until vehicle stopped. For this process, braking distance is 79.37 m, and braking time is 5.11 s, which meets the requirements of changing from pavement covered by snow to bitumen pavement.

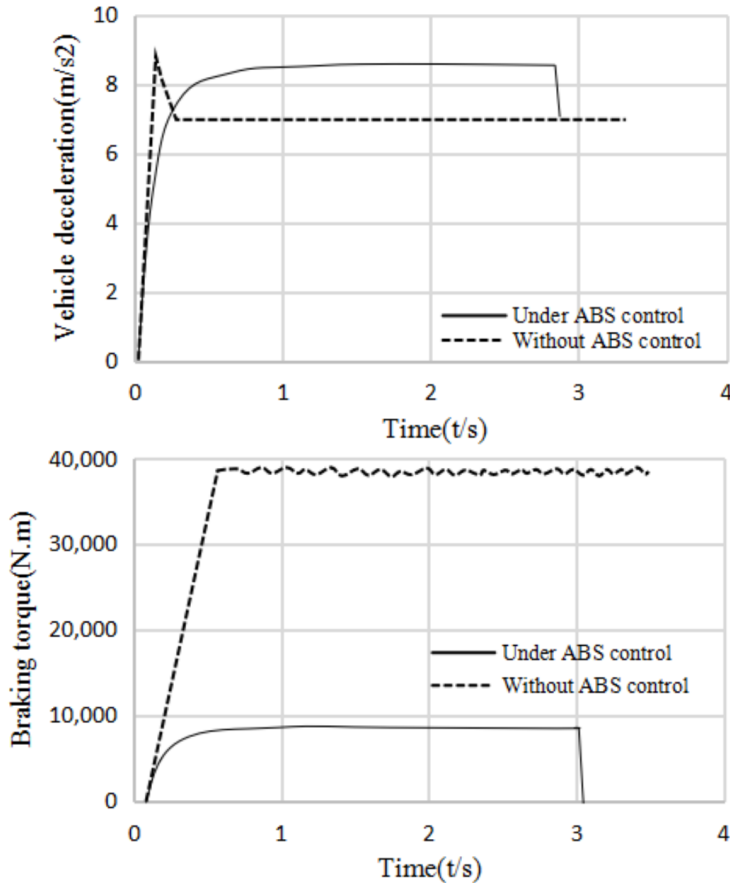


Fig. 7. Vehicle deceleration (up) and braking torque (bottom) for system with self-tuning fuzzy PID control and system without ABS control

6. Conclusion

This study is based on structure of braking system and braking methods, and below are the main research contents: EMB braking system model, tire model and single wheel vehicle model are built based on stress analysis of braking vehicle. Effectiveness of EMB braking system is verified that it met national standards for braking system. Improved self-tuning fuzzy PID controller is designed. And simulation results show that self-tuning fuzzy PID controller can adjust automatically according to external changes, which solves parameter setting problem of PID con-

troller because PID controller is nonlinearity and its parameters are changing with time. Adaptability of self-tuning fuzzy PID controller is verified by sudden changed pavement types. This simulation result shows that self-tuning fuzzy PID controller can control slip rate around target value, and identify optimal slip rate for different pavements, thus output of braking force is accurate controlled.

References

- [1] W. SHABIR, S. A. EVANGELOU: *Real-time control strategy to maximize hybrid electric vehicle powertrain efficiency*. *Applied Energy* 135 (2014), 512–522.
- [2] C. MONTERO, A. OLIVA, D. MARCOS, E. GONZÁLEZ, C. BORDONS, M. A. RIDAO, E. F. CAMACHO, E. LÓPEZ: *Fuel cell and power control for a hybrid vehicle. Experimental results*. Proc. Annual Conference on IEEE Industrial Electronics Society (IECON), 25–28 October 2012, Montreal, Québec, Canada, IEEE Conference Publications (2012), 4121–4126.
- [3] F. S. AHMED, S. LAGHROUCHE, M. EL BAGDOURI: *Analysis, modeling, identification and control of pancake DC torque motors: Application to automobile air path actuators*. *Mechatronics* 22 (2012), 195–212.
- [4] X. ZHU, H. ZHANG, D. CAO, Z. FANG: *Robust control of integrated motor-transmission powertrain system over controller area network for automotive applications*. *Mechanical Systems and Signal Processing* 58–59 (2015), 15–28.
- [5] J. B. ZHAO, B. ZHOU, S. Y. BEI: *Bang-Bang-PID control of automotive EPS system under damping condition*. *Electric Machines and Control* 15 (2011), No. 11, 95–100.
- [6] J. B. ZHAO, B. ZHOU, X. L. LI, S. Y. BEI: *Switched control strategy and performance test of electric vehicle electric power steering system under different conditions*. *Electric Machines and Control* 17 (2013), No. 11, 105–109.
- [7] S. DI CAIRANO, J. DOERING, I. V. KOLMANOVSKY, D. HROVAT: *Model predictive control of engine speed during vehicle deceleration*. *IEEE Transactions on Control Systems Technology* 22 (2014), No. 6, 2205–2217.
- [8] X. Q. ZHANG, B. YANG, C. YANG, G. N. XU: *Research on ABS of multi-axle truck based on ADAMS/car and Matlab/Simulink*. *Procedia Engineering* 37 (2012), 120–124.
- [9] H. ALIPOUR, M. B. B. SHARIFIAN, M. SABAHI: *A modified integral sliding mode control to lateral stabilisation of 4-wheel independent drive electric vehicles*. *International Journal of Vehicle Mechanics and Mobility* 52 (2014), No. 12, 1584–1606.
- [10] V. R. APAROW, F. AHMAD, K. HUDHA, H. JAMALUDDIN: *Modelling and PID control of antilock braking system with wheel slip reduction to improve braking performance*. *International Journal of Vehicle Safety* 6, (2013), No. 3, 265–296.
- [11] M. DEMIRCI, M. GOKASAN: *Adaptive optimal control allocation using Lagrangian neural networks for stability control of a 4WS-4WD electric vehicle*. *Transactions of the Institute of Measurement and Control* 35 (2013), No. 8, 1139–1151.
- [12] C. LV, J. ZHANG, Y. LI, Y. YUAN: *Mode-switching-based active control of power train system with nonlinear backlash and flexibility for electric vehicle during regenerative deceleration*. *Proceedings of the Institution of Mechanical Engineers Part D: Journal of Automobile Engineering* 229 (2015), No. 11, 1429–1442.
- [13] B. LONG, S. T. LIM, H. R. JI, K. T. CHONG: *Energy-regenerative braking control of electric vehicles using three-phase brushless direct-current motors*. *Energies* 7 (2014), No. 1, 99–114.
- [14] S. YU, C. MAIER, H. CHEN, F. ALLGÖWER: *Tube MPC scheme based on robust control invariant set with application to Lipschitz nonlinear systems*. *Systems & Control Letters* 62 (2013), No. 2, 194–200.
- [15] Y. LIU, L. Q. JIN, X. L. LIANG, Z. A. ZHENG: *Research on BP based fuzzy-PID controller for anti-lock braking system*. *Applied Mechanics and Materials* 365–366 (2013), 401–406.

- [16] V. R. APAROW, K. HUDHA, F. AHMAD, H. JAMALUDDIN: *Development of antilock braking system using electronic wedge brake model*. Journal of Mechanical Engineering and Technology 6 (2014), No. 1, 37–63.
- [17] G. YIN, X. J. JIN: *Cooperative control of regenerative braking and antilock braking for a hybrid electric vehicle*. Mathematical Problems in Engineering (2013), No. 4, paper 890427.
- [18] K. BAYAR, G. RIZZONI, J. WANG: *Development of a vehicle stability control strategy for a hybrid electric vehicle equipped with axle motors*. Proceedings of the Institution of Mechanical Engineers, Part D: Journal of Automobile Engineering 226 (2012), No. 6, 795–814.

Received May 7, 2017